

Energetics and mechanics of human running on surfaces of different stiffnesses

AMY E. KERDOK,^{1,2} ANDREW A. BIEWENER,³ THOMAS A. McMAHON,^{1,2†}
PETER G. WEYAND,^{3,4} AND HUGH M. HERR^{1,5,6}

¹Harvard Division of Health Sciences and Technology, and ⁵Artificial Intelligence Laboratory, Massachusetts Institute of Technology, Cambridge 02138; ³Concord Field Station, Museum of Comparative Zoology, Harvard University, Bedford 01730; ²Division of Engineering and Applied Sciences, Harvard University, Cambridge 02138; ⁴United States Army Research Institute for Environmental Medicine, Natick 01760; and ⁶Department of Physical Medicine and Rehabilitation, Harvard Medical School, Spaulding Rehabilitation Hospital, Boston, Massachusetts 02114

Received 12 December 2000; accepted in final form 24 September 2001

Kerdok, Amy E., Andrew A. Biewener, Thomas A. McMahon, Peter G. Weyand, and Hugh M. Herr. Energetics and mechanics of human running on surfaces of different stiffnesses. *J Appl Physiol* 92: 469–478, 2002; 10.1152/jappphysiol.01164.2000.—Mammals use the elastic components in their legs (principally tendons, ligaments, and muscles) to run economically, while maintaining consistent support mechanics across various surfaces. To examine how leg stiffness and metabolic cost are affected by changes in substrate stiffness, we built experimental platforms with adjustable stiffness to fit on a force-plate-fitted treadmill. Eight male subjects [mean body mass: 74.4 ± 7.1 (SD) kg; leg length: 0.96 ± 0.05 m] ran at 3.7 m/s over five different surface stiffnesses (75.4, 97.5, 216.8, 454.2, and 945.7 kN/m). Metabolic, ground-reaction force, and kinematic data were collected. The 12.5-fold decrease in surface stiffness resulted in a 12% decrease in the runner's metabolic rate and a 29% increase in their leg stiffness. The runner's support mechanics remained essentially unchanged. These results indicate that surface stiffness affects running economy without affecting running support mechanics. We postulate that an increased energy rebound from the compliant surfaces studied contributes to the enhanced running economy.

biomechanics; locomotion; leg stiffness; metabolic rate

IN THEIR GROUNDBREAKING work, McMahon and Greene (29) investigated the effects of surface stiffness (k_{surf}) on running mechanics. Their study sought to determine whether it was possible to build a track surface that would enhance performance and decrease injury. Their work showed that a range of k_{surf} values existed over which a runner's performance was enhanced by decreasing foot-ground contact time (t_c), decreasing the initial spike in peak vertical ground reaction force (f_{peak}), and increasing stride length. Tracks built within this enhanced performance range at Harvard University, Yale University, and Madison Square Garden have been shown to increase running speeds by

2–3% and to decrease running injuries by 50% (29). Despite the success of these “tuned tracks,” the mechanisms underlying the performance enhancement are not clearly understood.

A major assumption of McMahon and Greene's (29) was that the running leg and surface could be represented as a simple spring and mass (Fig. 1). McMahon and Cheng (27) subsequently described the leg spring as having two stiffnesses: k_{leg} and k_{vert} . The k_{leg} is the actual leg stiffness describing the mechanical behavior of the leg's musculoskeletal system during the support phase and is calculated from the ratio of f_{peak} to the compression of the leg spring (Δl , defined in Eq. B4)

$$k_{\text{leg}} = \frac{f_{\text{peak}}}{\Delta l} \quad (1)$$

In distinction, k_{vert} is the effective vertical stiffness of the runner. This stiffness serves as the mechanism by which the direction of the downward velocity of the body is reversed during limb contact (27, 30). Therefore, k_{vert} describes the vertical motions of the center of mass during the ground contact phase (27, 30). The k_{vert} can be calculated from the ratio of f_{peak} to the maximum vertical displacement of the center of mass during contact (Δy_{total}), measured from the onset of limb contact (heel-strike) to midstep

$$k_{\text{vert}} = \frac{f_{\text{peak}}}{\Delta y_{\text{total}}} \quad (2)$$

Farley et al. (12) and He et al. (19) determined that, for a given ground stiffness, k_{leg} changes little with speed. Later experiments showed that k_{leg} changes when animals run on surfaces of different stiffnesses (16, 18). It was specifically shown that human hoppers' k_{leg} adjustments were mainly due to changes in both ankle joint stiffness and leg posture (14). However, Aramatzis et al. (3) provided evidence that the knee joint is

†Deceased 14 February 1999.

Address for reprint requests and other correspondence: A. E. Kerdok, Harvard University, 29 Oxford St., Pierce Hall G-8, Cambridge, MA 02138 (E-mail: kerdok@fas.harvard.edu).

The costs of publication of this article were defrayed in part by the payment of page charges. The article must therefore be hereby marked “advertisement” in accordance with 18 U.S.C. Section 1734 solely to indicate this fact.

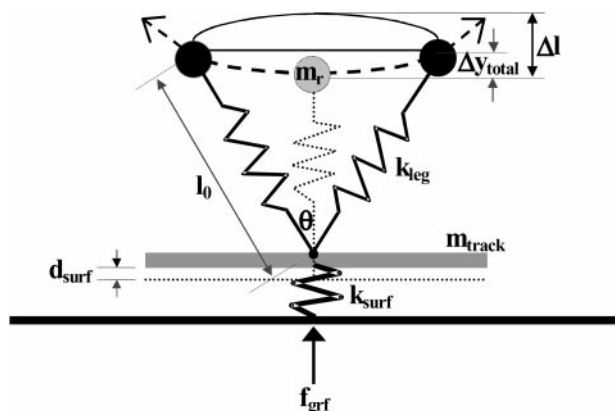


Fig. 1. Spring-mass model representing a runner's leg in contact with a compliant surface. l_0 , Uncompressed leg length; m_r , mass of the runner represented as a point mass located at the hip; Δy_{total} , maximum vertical displacement of the center of mass; Δl , maximum compression of the leg spring; θ , angle of the leg spring at first ground contact; k_{leg} , spring constant of the runner's leg; m_{track} , effective mass of the running surface; d_{surf} , amount the running surface deflects; k_{surf} , spring constant of the running surface; and f_{grf} , vertical ground reaction force.

the main determinant of k_{leg} as a function of speed in human running. In addition, modeling efforts and experiments on humans have shown that a runner's center of mass deflections (Δy_{total}) remain nearly constant, independent of k_{surf} , and that this may be a general principle of running mechanics (16, 29). In other words, by adjusting their "leg spring" stiffness to adapt to different k_{surf} values, a runner may be able to maintain apparently uniform support mechanics.

Representations of the running leg as a simple spring have described the mechanics of a running leg remarkably well (2, 11, 12, 15, 16, 18, 19, 25–27). It has been shown that the physical musculoskeletal elastic components of the leg (tendons, ligaments, and muscles) are used to minimize metabolic cost while running (1, 2, 8–10). However, no one, to date, has related the performance enhancements of running on surfaces of different stiffnesses to metabolic cost. In this paper, we assume that the leg can be represented by an undamped, linear spring and examine how the energetics and mechanics of running vary on surfaces of different stiffnesses.

The goal of this study is to relate human running biomechanics to energetics on surfaces of different stiffnesses. We expect that differences in the metabolic cost of running on various surfaces are likely related to the k_{leg} variations observed by Farley et al. and Ferris et al. (13, 17, 18). Specifically, we expect a less flexed knee to account for a reduction in metabolic cost (30), as well as an increase in k_{leg} (3, 18).

In this study, we investigate the energetics and mechanics of running on surfaces having a stiffness range from 75 to 945 kN/m. This range of stiffnesses was selected to incorporate the range of McMahon and Greene's "tuned track" (29) and to extend the work of similar recent studies (16–18). We hypothesize that the metabolic cost of forward human running reaches a minimum when the k_{leg} of the runner is maximized on

surfaces of decreased stiffness. We expect a cost reduction to result from a change in leg posture, whereby the knee is less flexed or straighter during stance (30). Running with a straighter leg should improve the limb's mechanical advantage, thereby reducing the amount of muscle force and muscle volume recruited to support body weight (5). We also anticipate that a reduction in metabolic cost could result from an increased energy return to the runner from the more compliant surfaces (14). Last, we expect that the runner's support mechanics will remain virtually unaffected across the above-defined range of k_{surf} .

EXPERIMENTAL METHODS

General procedures. Eight healthy male subjects [body mass: 74.4 ± 7.1 (SD) kg; leg length: 0.96 ± 0.05 m] ran at 3.7 m/s on a level treadmill, fitted with track platforms of five different stiffnesses (see descriptions below). All subjects wore the same flat-soled running shoes. Approval was granted from Harvard University's Committee on the Use of Human Subjects in Research, and subjects provided signed, informed consent before participation. Subjects ran for 5 min on each track platform stiffness in a mirrored fashion (running on stiffest to least stiff and then least stiff to stiffest). Beaded strings hung from the ceiling to give the runner a tactile sign as to where he needed to run so that his midstep corresponded with the fore-aft center of the track platform. Video was also used to ensure that the runner was both centered and lateral enough not to be stepping on both sides of the track simultaneously. If a runner was unable to avoid the seam between tracks, he was asked to move laterally and run on one track or the other. We recorded ground reaction force (1,000 Hz) using a force plate (model OR6–5-1, Advanced Medical Technology, Newton, MA) mounted within the treadmill (22). Kinematic data were collected at 60 Hz using an infrared motion analysis system (MacReflex by Qualysis), and oxygen uptake was measured using a closed gas-collection Douglas bag setup. Oxygen and carbon dioxide contents of the collected gas samples were analyzed using Ametek (Pittsburgh, PA) S-3A O₂ and CD-3A CO₂ analyzers equipped with an Ametek CO₂ sensor (P-61B) and flow controller (R-2). The analyzers were calibrated before each run with gas by pumping several balloons of known gas mixture (16.23% O₂ and 4.00% CO₂ medical gas mixture; AGA Gas, Billerica, MA) through them. Force-plate and kinematic data were obtained simultaneously, and oxygen consumption (V_{O₂}) data were sampled during the fourth and fifth minutes of running to ensure that the subject was at a steady state. Subjects participated in two separate trials so that they ran on each platform stiffness four times. Averages were taken on each day and then averaged together for all variables measured.

Experimental platform design. We built platforms with an adjustable stiffness for our running surface. Because the experiments were conducted on a treadmill, the running surface was limited to platforms that would fit within the size limitations of the treadmill. We used a treadmill fitted with an AMTI force plate (22) that was accessible to the Douglas bag oxygen analysis setup.

We tested five k_{surf} based on ranges found in the literature (14, 16, 18, 29). The McMahon and Greene (29) tuned track stiffness range is between 50 and 100 kN/m. Because of size limitations of the existing treadmill and earlier work done by Farley and Morgenroth (15) and Ferris et al. (17), we designed our variable stiffness track platforms to span from

75.4 kN/m to stiffnesses of 97.5, 216.8, 454.2, and 945.7 kN/m. The indoor track at Harvard University has a k_{surf} of ~ 190 kN/m, allowing for a 9-mm deflection for a 75-kg runner (assuming a runner exerts roughly 2.3 times body weight at midstance). For a similar runner, our track would result in 22.4-, 17.4-, 7.8-, 3.7-, and 1.8-mm deflections [surface deflections (d_{surf})], respectively, according to the following equation

$$d_{surf} = \frac{2.3 \cdot m_r \cdot g}{k_{surf}} \quad (3)$$

where m_r is the mass of the runner, g is the gravitational constant, and k_{surf} is the stiffness of the track. The factor 2.3 is an estimate of how much the f_{peak} exceeds body weight during a running step.

The platform design is shown in Fig. 2. Garrolite (G-10, Current, East Haven, CT) was chosen as the material for the track platforms because it met all of the design criteria described below and in APPENDIX A and could be easily machined. The design consisted of two G-10 planks ($1.22 \times 0.254 \times 0.014$ m) rigidly supported in the front and simply supported in the rear by 0.016-m-thick acrylic. By moving the treadmill rollers in at either end of the belt surface, enough slack was provided to fit the platforms under the belt directly on top of the force plate. Rollers were added to the existing treadmill to reroute the treadmill belt over the platforms, and a frame was built (not shown) to hold the platform in place on top of the force plate during testing. The rear support was movable so that, by simply adjusting it in closer to or farther away from the front support, the stiffness of the running surface was increased or decreased, respectively.

Once installed, the stiffness of each platform was calibrated by applying static loads to a person and measuring force (f_{peak} , from the force plate) and deflection (d_{surf} , from an LVDT cable extender $\pm 0.25\%$, Celesco Transducer Products) (Eq. 3).

As described in APPENDIX A, the inertial effects of the running platform motion compared with the forces exerted by the runner's leg can be considered negligible if the effective mass of the platform is $<17\%$ of the m_r (11.43 kg for the smallest runner studied). The effective masses (6.88, 8.88, 4.94, 2.65, and 5.39 kg) gave inertial forces of -41.43 , -30.41 , -10.04 , -3.33 , and -0.42 N, respectively. These forces were $<2.5\%$ of the peak forces exerted by the runner and so were ignored.

Given that the running surface was a compliant surface having the potential to return energy to the runner, we also

calculated the energy return of our variable-stiffness track platform. We did this by using the track deflection to derive the potential energy at each track stiffness (E_{track})

$$E_{track} = \frac{1}{2} k_{surf} d_{surf}^2 \quad (4)$$

Multiplying this energy by two times the stride frequency results in the mechanical power delivered from the track to the runner. This was then related to a measurement of the metabolic power (E_{metab}) consumed by the runner at each track stiffness.

Force-plate measurements. A runner's support mechanics, defined as f_{peak} , t_c , duty factor, stride frequency, step length, one-half of the angle swept by a runner's leg during ground contact (θ), and the total vertical displacement of the center of mass, can be calculated from the force-plate data and the assumption that the leg can be represented by an undamped, linear spring (22). These parameters can then be indirectly used to calculate the mass-spring characteristics of the runner's leg. Custom LabVIEW (version 4.0.1) software was used to acquire the force-plate data. The force plate was calibrated by applying known loads to the plate before and after each set of running trials and sampling its output using the same software. The derivation of all of the above parameters is described in APPENDIX B.

Kinematic measurements. To obtain information on the posture of the limb in contact with the ground, we used an infrared camera system (MacReflex; Qualysis) to follow markers that were specifically placed on the subjects. Markers were positioned on the skin overlying the greater trochanter, the lateral epicondyle of the femur, and the lateral malleolus, so that the angle that the lower leg made with the upper leg (knee angle) could be determined.

Kinematic data were collected simultaneously and synchronized with the force-plate data (using an infrared light-emitting diode in the camera's field of view that gave a voltage pulse that was recorded when the light-emitting diode was switched on). Kinematic data were analyzed using the Maxdos software from MacReflex (Qualysis) and incorporated into a Matlab (version 4.0) program to calculate the knee angle at midstep. The program also calculated the series minimum height points of the greater trochanter marker for several strides over the 10-s collection period. This marker was used to estimate the position of a runner's center of mass, and its minimum trajectory was used to define the midpoint of each step when force application reached its peak (13, 19, 26).

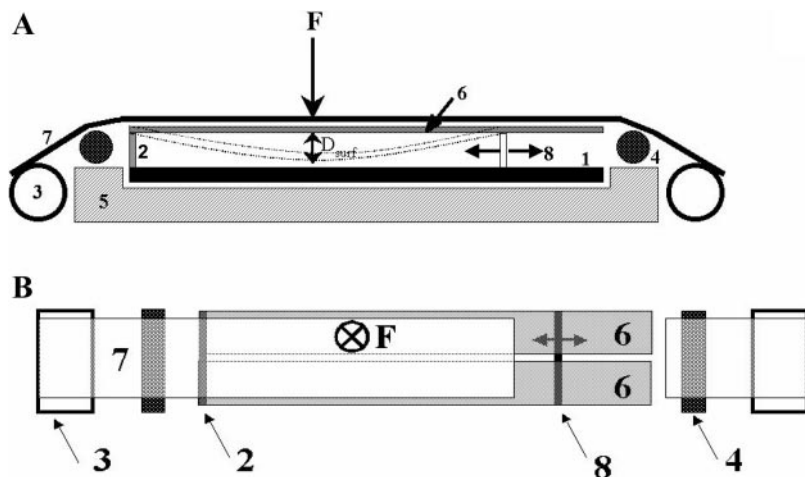


Fig. 2. Side view (A) and top view (B) of a schematic of the experimental compliant track treadmill. The runner's foot strikes the treadmill belt (7) (note that this is cut away on top view to show underlying structures and also that the belt is longer than depicted) and exerts a vertical force (F) on the compliant running platforms (6) below. The vertical force is transmitted from the platforms via the supports (2 and 8) to the force plate (1). The stiffness of the running surface is adjusted by moving the movable support (8) in and out. The force plate (1) and entire treadmill apparatus are supported by the treadmill base (5). By moving the treadmill rollers (3) closer together, enough slack is recovered in the belt (7) to insert the track platforms (6). The belt is then redirected over the track platforms with the redirection rollers (4).

Measuring metabolic cost. To quantify the metabolic cost of human running, we used the indirect calorimetry method, as described previously. After the runners ran for 3 min, we collected the expired air for 2 min using two Douglas bags (1 per minute), a mouthpiece, and a nose clip, which were attached to the runner via a special headpiece equipped with a one-way valve. The rate of $\dot{V}O_2$ (ml/min) was then calculated using the volume of the expired air (from a dry-gas volume meter; Parkinson-Cowan), room and vapor pressure corrections, and the percentage of CO_2 and O_2 values. We converted the rate of $\dot{V}O_2$ into energy consumption using an energy equivalent of 20.1 J/ml O_2 (6) and divided by 60 s/min to obtain \dot{E}_{metab} in watts.

Kram and Taylor (23) define the rate of metabolic consumption (\dot{E}_{metab}) in terms of a cost coefficient, C_0

$$\dot{E}_{metab} = C_0 \left(\frac{1}{t_c} \right) (F_{bw}) \quad (5)$$

where C_0 is an empirical measure of the metabolic cost of applying ground force to support the body's weight (F_{bw}) (4, 31). For this investigation, the C_0 is computed to determine the effect of k_{surf} on the energetics of supporting the runner's body weight.

Statistical methods. A 1×5 ANOVA with a Scheffé post hoc test of condition means was used to assess the effect of k_{surf} on the parameters of interest: t_c , peak vertical force, stride time, stride frequency, step length, θ , Δy_{total} , displacement of the limb with respect to the track displacement, \dot{E}_{metab} , C_0 , k_{leg} , k_{vert} , Δl , overall system stiffness, and knee

angle. P values <0.05 were considered significant for all tests.

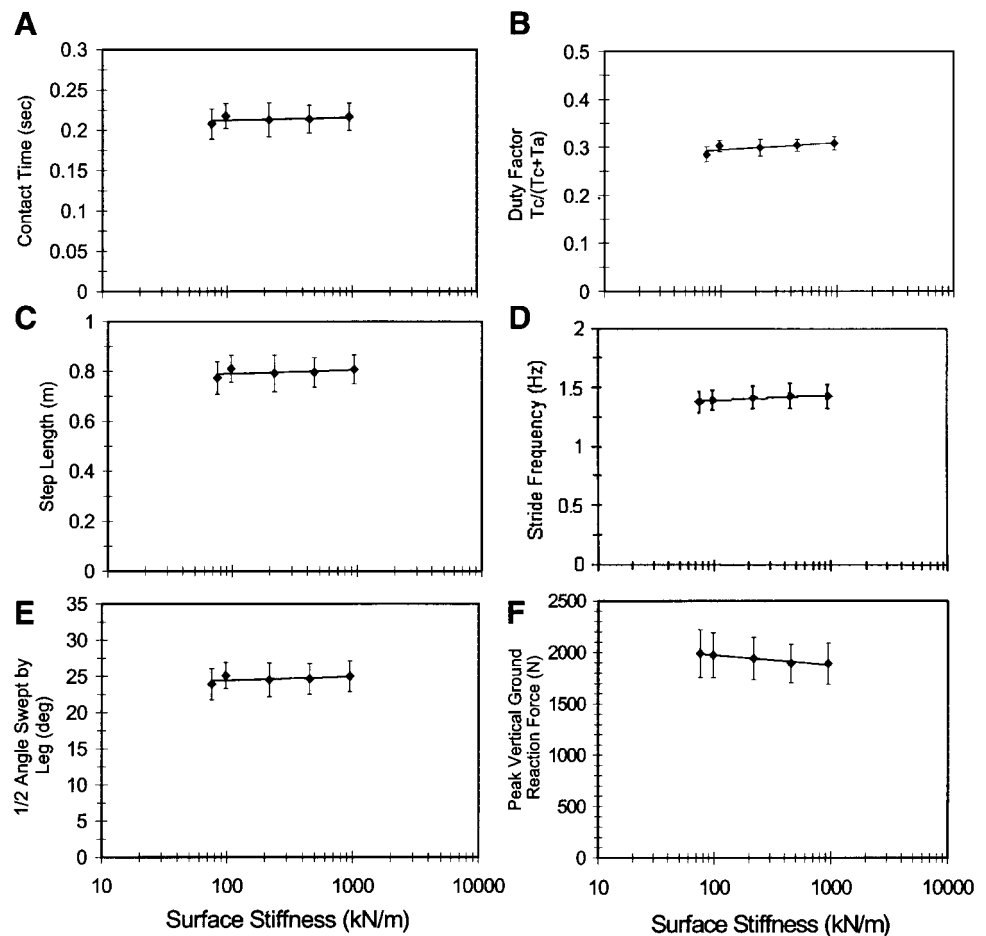
RESULTS

The runner's support mechanics were nearly invariant across the 12.5-fold change in k_{surf} of the experimental treadmill platform (Fig. 3), whereas their metabolic rate dropped dramatically with k_{surf} (Fig. 6).

The results of the Scheffé post hoc test revealed that, in virtually every case, the support mechanics remained essentially unchanged over the four stiffest surfaces tested. The basis for a significant difference in the ANOVA results reported below was found to be due to the data recorded for the lowest stiffness track surface.

As shown in Fig. 3, the effect of k_{surf} on t_c ($P = 0.0001$, $F = 8.7$), duty factor ($P = 0.0001$, $F = 18.45$), step length ($P = 0.0001$, $F = 8.51$), stride frequency ($P = 0.0001$, $F = 15.35$), θ ($P = 0.0001$, $F = 8.44$), and f_{peak} ($P = 0.009$, $F = 4.19$) were significant. However, the data across these support mechanics showed only a small difference between the two stiffness extremes. The source of the difference occurred at the lowest stiffness, with the remaining four stiffnesses being essentially the same.

Fig. 3. When subjects ran at a constant speed (3.7 m/s) over 5 different surface stiffnesses (74–945 kN/m), their support mechanics remained essentially unchanged. As confirmed by the Scheffé post hoc test, the differences observed were due to the lowest surface stiffness only. The time that the foot is in contact with the ground [$y = 0.0017 \ln(x) + 0.204$, $R^2 = 0.21$] (A); the duty factor [$y = 0.0063 \ln(x) + 0.265$, $R^2 = 0.58$] (B); the step length (right foot to left foot) [$y = 0.0065 \ln(x) + 0.76$, $R^2 = 0.22$] (C); the stride (right foot to right foot) frequency [$y = 0.019 \ln(x) + 1.31$, $R^2 = 0.87$] (D); the angle swept by the runner's leg [$y = 0.221 \ln(x) + 23.44$, $R^2 = 0.24$] (E), and the peak vertical ground reaction force [$y = -41.4 \ln(x) + 2163.2$, $R^2 = 0.94$] (F) were all virtually constant. Values are means \pm SD. T_c , period of foot-ground contact; T_a , period of foot in air.



In particular, when the support mechanics means are compared, there was a 4% decrease in t_c , step length, and θ between the stiffest and least stiff surfaces studied. A 7% decrease in duty factor, 3% decrease in stride frequency, and a 5% increase in f_{peak} were also observed between these stiffness extremes.

The post hoc test revealed that the runners also maintained a nearly constant total leg plus track platform stiffness (k_{totL}) over the observed range of conditions ($P = 0.0207, F = 3.45$) (Fig. 4C). To achieve this, the runner's k_{leg} increased by 29% with decreasing k_{surf} ($P = 0.0001, F = 23.76$) (Fig. 4A). Given that the runner's f_{peak} did not change greatly over the substrate stiffness range (Fig. 3F), the observed increase in the runner's k_{leg} most likely resulted from a decrease in the amount that his leg spring was compressed ($P = 0.0001, F = 33.93$) (Eq. 1, Figs. 1 and 4D). The Δl is a function of leg length, θ , and vertical displacement of the runner relative to the displacement of the track surface (y_{limb}) (Eq. B4). Because leg length and θ remained essentially constant, the decrease in the Δl was likely due to the observed decrease in y_{limb} ($P = 0.0001, F = 94.05$) (Fig. 5B, Eq. B5).

We achieved the five different k_{surf} by allowing the simply supported track to displace beneath the runner. Therefore, d_{surf} increased 12.5-fold from the stiffest to the least stiff surface (Fig. 5A). This substantial increase in surface displacement was mostly offset by y_{limb} so that y_{total} was minimally changed between the k_{surf} extremes (~ 0.8 cm) ($P = 0.0001, F = 16.28$). Again, the change in y_{total} was only significant at the lowest k_{surf} studied (Fig. 5C). Our finding that the k_{vert} (Fig. 4B) remained virtually constant ($P = 0.0001, F = 11.77$) over the four stiffest surfaces further supports the fact that the runners' Δy_{total} changed minimally, as k_{vert} is a function of f_{peak} and y_{total} . (Eq. 2).

We also found a 12% decrease in the runner's rate of \dot{E}_{metab} as k_{surf} decreased ($P = 0.0001, F = 71.95$) (Fig. 6A). The runner's mean \dot{E}_{metab} decreased from 896 to 792 W as k_{surf} decreased from 945 to 75 kN/m. Referring to Eq. 5 and recalling that t_c remained essentially unchanged (Fig. 3A), the observed decrease in metabolic rate suggests that the C_0 defined by Kram and Taylor (23) also decreased with decreasing k_{surf} ($P = 0.0001, F = 32.54$) (Fig. 6B).

In an attempt to evaluate limb mechanical advantage, we used the kinematic data, together with the vertical ground reaction force, to calculate the limb's knee angle at midstep for running over all surfaces (Fig. 7). Knee angle increased 2.5% as k_{surf} decreased ($P = 0.0001, F = 16.35$). Thus only a slight straightening of the leg was observed.

Last, to test our hypothesis that the track itself may return significant energy to the runner, we calculated the track platform's mechanical power (E_{track} , Eq. 4) at each k_{surf} and compared this with the reduction in \dot{E}_{metab} of the runner (Eq. 5) (Fig. 8). The results show that, for every watt of mechanical power returned from the track platform, there exists the possibility of a 1.8-W \dot{E}_{metab} savings to the runner ($R^2 = 0.99$).

DISCUSSION

Our results support the hypothesis that the metabolic cost of running at an intermediate speed is progressively reduced and that the spring stiffness of the leg is progressively increased as k_{surf} is decreased from 945.7 to 75.4 kN/m. However, in contrast to our hypothesis that a change in limb posture is the principal factor underlying a change in both k_{leg} and metabolic cost, we found that only small changes in knee angle were associated with the observed 29% increase in k_{leg} and 12% decrease in \dot{E}_{metab} . Our data do not provide

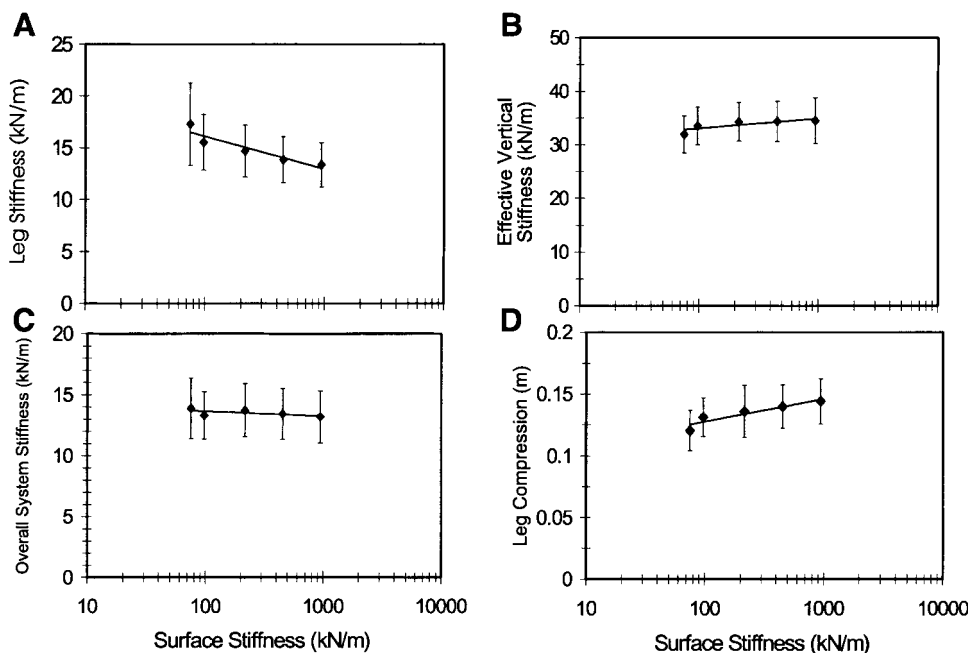


Fig. 4. When subjects ran at a constant speed (3.7 m/s) over 5 different surface stiffnesses (74–945 kN/m), there was a 29% change in their leg stiffness [$y = -1.37 \ln(x) + 22.4, R^2 = 0.87$] (A) and a 16% decrease in leg compression [$y = 0.008 \ln(x) + 0.091, R^2 = 0.86$] with decreasing surface stiffness (D). The overall stiffness of the system [$y = -0.175 \ln(x) + 14.46, R^2 = 0.4$] (C) and the effective vertical stiffness of the runner [$y = 0.81 \ln(x) + 29.31, R^2 = 0.66$] (B) remained essentially unchanged. Values are means \pm SD.

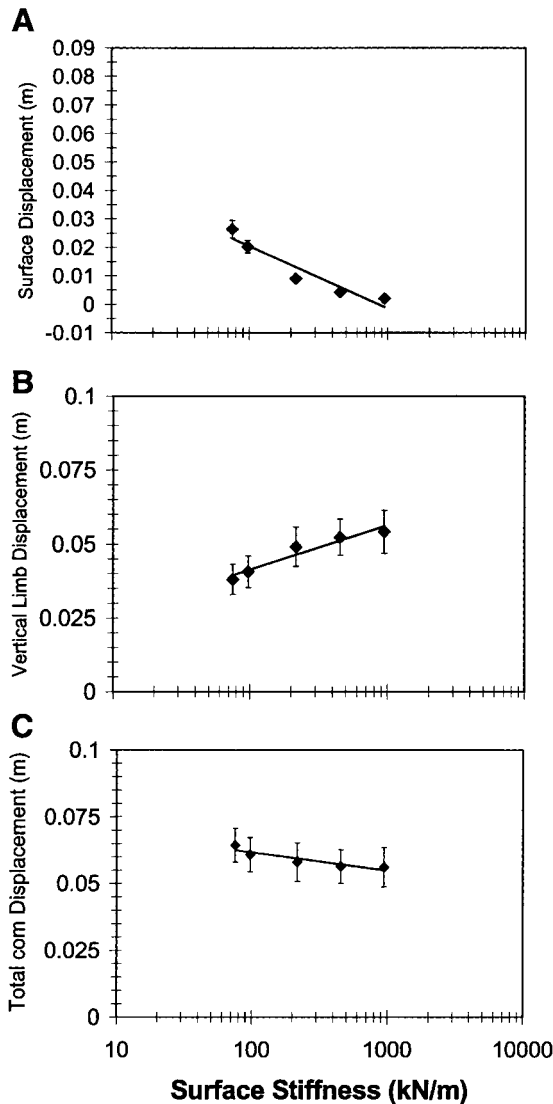


Fig. 5. A: as designed, the vertical displacement of the compliant running surface increased with decreasing surface stiffness [$y = -0.01 \ln(x) + 0.064, R^2 = 0.91$]. B: the vertical displacement of the runner's center of mass relative to the track's vertical displacement decreases with surface stiffness [$y = 0.0065 \ln(x) + 0.011, R^2 = 0.93$]. This limb displacement is used to define the leg compression (Fig. 4, Eq. B4), which in turn defines the leg stiffness of the runner (Fig. 4, Eq. 1). C: the total vertical displacement of the runner's center of mass (com) measured from midstep to take-off using the vertical displacement of the hip marker is essentially unchanged over the surface stiffnesses [$y = -0.003 \ln(x) + 0.076, R^2 = 0.84$]. This value is used to define the effective vertical stiffness (Fig. 4, Eq. 2). Values are means \pm SD.

any additional insight into the mechanism for k_{leg} adjustment but do suggest that a reduction in metabolic cost occurs as the elastic rebound provided by a more compliant surface replaces that otherwise provided by a runner's leg.

Previous work indicated that runners adjust the stiffness of their limbs to maintain virtually constant support mechanics on surfaces of different stiffnesses (3, 14, 16, 18, 28). Although these studies provide insight into the mechanics of human running, they did

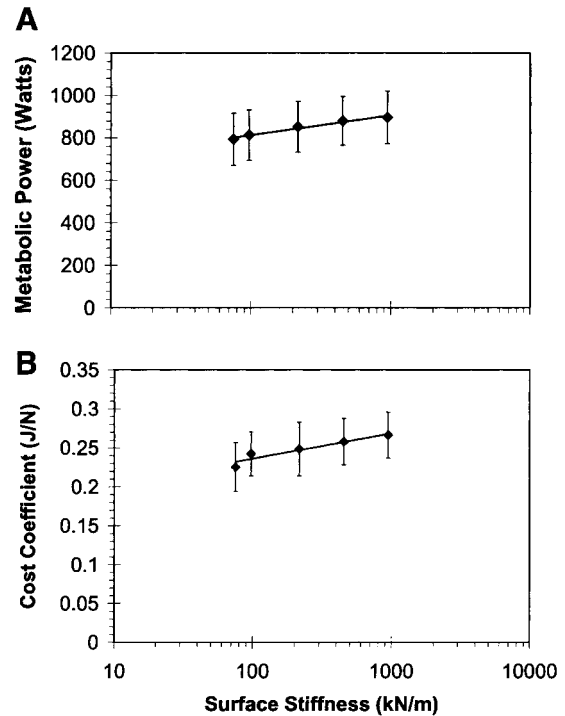


Fig. 6. A: the runner's metabolic rate decreased with surface stiffness [$y = 41.17 \ln(x) + 622.31, R^2 = 0.97$] over the 12.5-fold change in surface stiffness (74–945 kN/m) when running at a constant speed (3.7 m/s). B: because the contact time remained essentially constant (Fig. 3), the cost coefficient must also decrease with surface stiffness [$y = 0.0142 \ln(x) + 0.171, R^2 = 0.91$] per Eq. 5 [$\dot{E}_{metab} = C_0 \times (1/t_c) \times F_{bw}$, where \dot{E}_{metab} is the rate of metabolic consumption, C_0 is an empirical measure of the metabolic cost of applying ground force to support the body's weight (F_{bw}), and t_c is the period of foot-ground contact]. Values are means \pm SD.

not specifically examine the metabolic cost of running on compliant surfaces. One study (30) looked at deep-knee-flexed running and its effect on k_{vert} and $\dot{V}O_2$ but did not incorporate k_{leg} or compliant surfaces. Our goal was to expand on these earlier studies and examine how changes in limb-substrate stiffness interactions affect the metabolic cost of running. Consequently, we

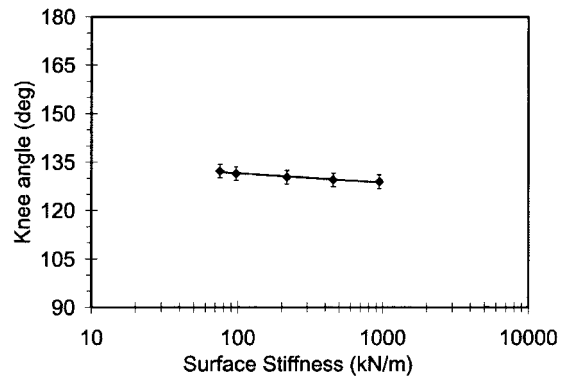


Fig. 7. The angle formed between the runner's upper and lower legs was defined from markers placed at the greater trochanter, lateral epicondyle of the femur, and lateral malleolus. This knee angle increased 2.5% as surface stiffness decreased [$y = -1.25 \ln(x) + 137.29, R^2 = 0.97$], giving rise to a slightly straighter leg on the softer surfaces studied. Values are means \pm SD.

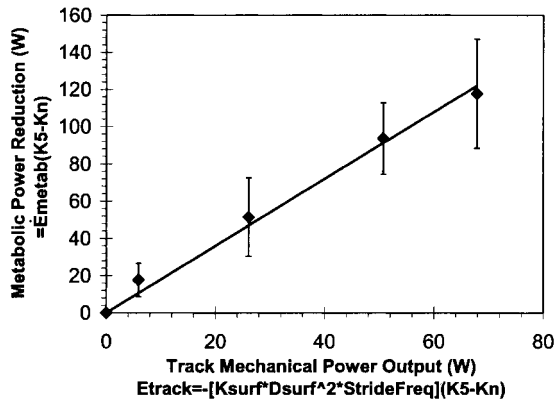


Fig. 8. Change in the runner’s metabolic power (\dot{E}_{metab}) as a function of the change in mechanical power delivered from the track platforms (E_{track}) from the stiffest surface (K_5). The power delivered from the compliant track is derived from the mechanical energy due to the track spring (Eq. 4) multiplied by the runner’s stride frequency. For every watt delivered from the track platforms, there exists a potential 1.8-W reduction in metabolic power ($y = 1.80x$, $R^2 = 0.99$). Values are means \pm SD. K_n , surface stiffness where $n = 1, 2, 3, 4$.

adopted a similar mechanical and experimental approach to that of these studies, focusing on the knee joint and assuming that the leg behaves as a massless, undamped linear spring.

Using this simple model of the human leg, our findings generally support those of Farley et al. (11, 13–15), indicating that human runners alter their leg spring stiffness to compensate for changes in k_{surf} without altering their overall support mechanics. McMahon and Greene (29), Farley et al. (14), and Ferris et al. (17) have commented that an observer looking only at the upper body of a runner would be unable to discern when the runner experienced a change in ground stiffness. This suggests that runners compensate for variable ground stiffness without affecting the fluctuations in the motion of their center of mass. This is consistent with our findings that d_{surf} is offset by y_{limb} , thus resulting in the minimal 0.8-cm change observed in y_{total} . Hence, utilizing preferred support mechanics might represent a general principle of running.

Kram and Taylor’s (23) analysis suggests that the mass-specific metabolic rates of running animals are determined by the rate of ground-force application ($1/t_c$), regardless of the speed and size of the animal. Their analysis assumes that animals maintain a uniform limb mechanical advantage over a range of running speeds and gaits. This assumption is supported by previous studies of animals moving at steady speeds over a constant (high) stiffness substrate (5). As a result, the cost of force generation and the volume of muscle that must be activated to support a given unit body weight also appear to remain constant (21). However, we found a reduction in metabolic rate with virtually no change in the t_c (Figs. 3A and 6A). Thus the energetic cost of applying a ground force to support the runner’s body weight can be reduced at a given rate of ground force application ($1/t_c$) when running on more compliant surfaces.

The close relationship between the reductions in metabolic rates and the increased mechanical power returned by the track to the runner in the latter portion of foot-ground contact (Fig. 8) offers a straightforward explanation. This close relationship strongly suggests that, when a greater share of the elastic rebound elevating the center of mass in the latter portion of the contact phase is provided by the elastic recoil of the running surface rather than the biological springs in the runner’s leg, the metabolic cost of running is reduced. We believe that these reductions in the metabolic cost of operating leg springs are probably explained by decreases in the mechanical work and shortening velocity performed by the muscles active during foot-ground contact.

Although we had hypothesized that reductions in metabolic cost and increases in k_{leg} would be achieved predominantly via changes in knee angle, it seems evident that this mechanism cannot fully account for these changes. The change in k_{leg} is likely due to a combination of local joint stiffness variation and overall limb posture adjustment (15). Whereas our study provided some indication that the leg becomes straighter at midstep on less stiff surfaces (Fig. 7), the change at the knee was small and would require a large sensitivity to have an effect on externally developed knee torque. Therefore, this small change in knee angle could only account for a minority of the reductions in metabolic cost and increases in k_{leg} that we observed on more compliant surfaces.

Our hypothesis also anticipated that the decrease in \dot{E}_{metab} might well be explained by an enhanced energy return from the more compliant track platforms. The elastic surface could actually be assisting the runner by assuming some of the cost necessary to operate the leg spring, reducing the amount of mechanical work required, and thereby allowing the leg muscles to operate more isometrically. Reductions in relative shortening velocities would reduce metabolic cost in two ways. First, the increased force per unit area of active muscle would reduce the volume of muscle required to support the body’s weight. Second, the \dot{E}_{metab} consumed per unit of active muscle is also reduced when the muscles shorten through a lesser distance (20).

To lend support for these ideas, experiments were conducted to characterize the track-runner interaction. The dynamic calibration of the four most compliant experimental track platforms showed a linear relationship between force and displacement ($R^2 = 0.96, 0.97, 0.95$, and 0.94 from least to most stiff) with little hysteresis (damping ratio < 0.1). Hence, the track can indeed be considered an elastic substrate capable of storing and returning mechanical energy. Also, by calculating the resonant period of the track-plus-runner system at the least stiff surface (~ 0.2 s) and comparing the result to the contact times of the runners at this same stiffness (0.21 ± 0.02 s), we conclude that the track has sufficient time to return its stored energy to the runner. Last, our results show a consistent linear

relationship between the reduction in \dot{E}_{metab} and track mechanical power output across all surfaces studied (Fig. 8). These results suggest that the track has the capacity to save the runner 1.8 W of \dot{E}_{metab} for every watt of mechanical power that it returns.

Although our results support the fact that running on a decreased k_{surf} results in a reduction of metabolic cost and an increase in k_{leg} without affecting support mechanics, future studies need to be done to find a true metabolic minimum. Our measurements were designed to examine surfaces that were within a stiffness range that had already demonstrated an enhanced running performance (29). However, support mechanics are progressively altered to accommodate extreme decreases in k_{surf} . As mentioned above, our results support our hypothesis that these support mechanics would remain fairly constant over the 12.5-fold change in k_{surf} but also show a significant change in these variables at the lowest k_{surf} studied. This raises the possibility of a trend in data as k_{surf} goes even lower. McMahon and Greene's (29) work supports this speculation. We also anticipate that, as k_{surf} decreases even further and the virtual consistency of the support mechanics seen at the higher stiffnesses is lost, there would exist a true metabolic minimum. Studies that looked at running on surfaces with extremely low stiffness, such as a trampoline and pillows (30) or sand (24), which also have high damping ratios, indicate that runners likely increase the amount of center-of-mass work that they perform and thus substantially increase their cost of locomotion (24). We propose that a study be done to examine lower k_{surf} values than were studied here to determine at what substrate stiffness a true metabolic minimum exists as a relation of speed. We believe that there exists an optimal ratio of t_c to surface resonant period that can be used for the future design of tracks and even running shoes to minimize the cost of running.

Summary. Our study sought to link the mechanics and energetics of human running on surfaces of different stiffnesses. The results show that both metabolic cost and k_{leg} change when k_{surf} is manipulated. The metabolic reduction is largely due to the track's elastic energy return assisting the runner's leg spring. Although the mechanism for k_{leg} adjustment still remains unclear, our results support the hypothesis that human runners adjust k_{leg} to maintain consistent support mechanics across different surfaces.

This study has served to link previous studies on animal locomotion and to open the door to future investigations on locomotory mechanics and energetics. Understanding how metabolism, speed, and k_{leg} relate to substrate mechanics will not only lead to advances in running shoe technology and track design, but may also motivate the development of highly adaptive orthotic and prosthetic leg devices that change stiffness in response to speed and ground surface variations, enabling the physically challenged to move with greater ease and comfort.

APPENDIX A

Experimental Track Platform Design

The design of the variable-stiffness track platform was based on simply supported, two-point bending beam theory. Pilot studies showed that this configuration would work well within the size limitations of the treadmill (0.102-m maximum height from the force plate to beneath the belt, 1.22-m long \times 0.457-m wide force plate, and 0.5 \times 2.64-m overall belt surface). Materials and dimensions were chosen based on the maximum deflection (y_{max}) of the center of the beam according to the factor of safety (FS) associated with the loads that would be applied in running (F) or

$$y_{\text{max}} = \frac{-FL^3}{48EI} \quad (A1)$$

$$\text{FS} = \frac{\sigma_u}{\sigma_{\text{max}}} \quad (A2)$$

where L is the length of the beam, E is Young's modulus, I is the area moment of inertia, σ_u is the ultimate stress of the material, and σ_{max} is the maximum allowable stress of the material.

Another design criterion was that the track platform mass needed to be small enough so that the inertial forces due to the movement of the platform would be negligible compared with the forces exerted by the runner's leg. By modeling the leg and platform surface as a two-mass and two-spring system with a damper, we found that the effective mass of the platform had to be <12 kg (or 17% of the m_r) in order for the platform's inertia to represent $<10\%$ of the peak force developed by a 72-kg runner. Therefore, given that the masses of the actual runners were from 67.3 to 81.5 kg, the effective mass of the track platforms (m_{track}) had to be <11.4 – 13.9 kg to meet this criterion.

The inertial effects of the track platforms on measurements obtained from the force plate could be obtained by calculating the effective mass of the platforms. The m_{track} was estimated by treating the track as a harmonic oscillator and finding the damped frequency (ω_d). The ω_d was measured by striking the platform and plotting the displacement vs. time for the free vibration of the track surface (14). This was accomplished by mounting the LVDT cable extender at the center edge of the platform for each stiffness configuration, with the platform resting in position on top of the AMTI force plate and under the treadmill belt. The ω_d was computed from the period of vibration (T_d) or

$$\omega_d = \frac{2\pi}{T_d} \quad (A3)$$

The equation describing the envelope of the free vibration curve can be used together with the damped natural frequency of the track to obtain the natural frequency and the damping ratio of the track surfaces

$$x = \pm Ae^{-\xi\omega_n t} \quad (A4)$$

$$\omega_d = \omega_n \sqrt{1 - \xi^2} \quad (A5)$$

where x defines the envelope of free vibration, A is the amplitude of free vibration, ω_n is the natural frequency, and t is time. With the use of Eqs. A4 and A5, the natural frequency of the platform was calculated to be 105 rad/s, thus resulting in a negligible damping ratio of $\xi \approx 0.07$. Hence the m_{track} was estimated from the k_{surf} and the ω_d , or

$$m_{\text{track}} \approx \frac{k_{\text{surf}}}{\omega_d^2} \tag{A6}$$

The m_{track} was then used, together with the second derivative of the displacement curves (to obtain acceleration), to estimate the inertial force (F_{inertial}) of the track platforms using

$$F_{\text{inertial}} = m_{\text{track}} \frac{d^2x}{dt^2} \tag{A7}$$

APPENDIX B

Derivation of the Force-Plate Parameters

LabVIEW (version 4.0.1) was used to acquire the force-plate data and output the parameters of the runner’s support mechanics (f_{peak} , t_c , stride time, stride frequency, step length, θ , and the vertical displacement of the center of mass). Because of the vibrational noise from the treadmill belt, motor, and track (22), we filtered the force data using a low-pass, third-order Butterworth double-reverse filter. The smoothed curve for the ground reaction force was used for analysis. The f_{peak} is the force at midstep and was taken to be the maximum value of this curve. The duration of the force provided a measure of the t_c as well as total stride (right foot to right foot) time ($t_c + t_a = \text{dur}_{\text{tot}}$, where t_a is the period the foot is in the air and dur_{tot} is total duration) that were then used to calculate the stride frequency (freq) and step length (SL) (distance traveled by the center of mass during one t_c)

$$\text{freq} = \frac{\text{Hz}}{\text{dur}_{\text{tot}}} \tag{B1}$$

$$\text{SL} = t_c \bar{u}_x \tag{B2}$$

where \bar{u}_x is the horizontal (forward) velocity. With the additional input of the runner’s leg length (l_o) measured from the runner’s greater trochanter to the floor while standing straight legged, we calculated θ (see Fig. 1) from

$$\theta = \sin^{-1} \left(\frac{\text{SL}}{2l_o} \right) \tag{B3}$$

Because the ground reaction force is equal to the runner’s m_r times his acceleration, we were able to calculate the Δy_{total} of the runner by twice integrating the vertical acceleration of the center of mass over time (7).

To account for the displacement of the variable-stiffness surfaces (d_{surf}) in relation to the runner’s Δy_{total} , we calculated d_{surf} from the calibrated values obtained for k_{surf} and the forces obtained from the force plate (Eq. 3, where $2.3 * m_r = f_{\text{peak}}$ from force plate).

The above variables were then used to calculate the mass-spring characteristics of the runner’s leg. The maximum Δl was calculated by using the runner’s l_o , θ , and the actual Δy_{limb} (18, 26)

$$\Delta l = \Delta y_{\text{limb}} + l_o(1 - \cos \theta) \tag{B4}$$

$$\Delta y_{\text{limb}} = \Delta y_{\text{total}} - d_{\text{surf}} \tag{B5}$$

Because the f_{peak} occurs at the same time that the center of mass is at its lowest height, the stiffness of the leg spring (k_{leg}) was calculated using the ratio of f_{peak} to maximum leg compression (13, 19, 26) (Eq. 1). Similarly, the effective vertical spring stiffness was calculated using the peak force and the total displacement of the center of mass of the system (Eq. 2).

The total displacement is used in calculating k_{vert} rather than the actual displacement of the runner alone, because, on less stiff surfaces, k_{vert} is affected by the displacement of the surface (18). If the actual (or relative) displacement is used, the possibility exists that vertical stiffness could assume a negative value (the runner moves in the opposite direction at midstep in an effort to maintain a constant displacement of the system’s center of mass), which is nonsensical.

Overall stiffness of the system (k_{totL}) was calculated as the sum of the k_{leg} and the track platform stiffness (k_{surf}) in series

$$\frac{1}{k_{\text{totL}}} = \frac{1}{k_{\text{leg}}} + \frac{1}{k_{\text{surf}}} \tag{B6}$$

The authors thank Claire Farley and Roger Kram from the University of California at Berkeley for helpful discussions, as well as Robert Wallace from the United States Army Research Institute for Environmental Medicine for statistical analysis.

This research was supported in part by a graduate fellowship from the Whitaker Foundation and the Division of Engineering and Applied Sciences, Harvard University.

REFERENCES

1. **Alexander RM.** *Elastic Mechanisms in Animal Movement.* Cambridge, UK: Cambridge University Press, 1988, p. 30–50.
2. **Alexander RM.** A model of bipedal locomotion on compliant legs. *Philos Trans R Soc Lond B Biol Sci* 338: 189–198, 1992.
3. **Arampatzis A, Bruggemann G, and Metzler V.** The effect of speed on leg stiffness depends on knee stiffness during human running. *J Biomech* 32: 1349–1353, 1999.
4. **Biewener AA.** Biomechanics of mammalian terrestrial locomotion. *Science* 250: 1097–1103, 1990.
5. **Biewener AA.** Scaling body support in mammals: limb posture and muscle mechanics. *Science* 245: 45–48, 1989.
6. **Blaxter K.** *Energy Metabolism in Animals and Man.* Cambridge, UK: Cambridge University Press, 1989.
7. **Cavagna GA.** Force platforms as ergometers. *J Appl Physiol* 39: 174–179, 1975.
8. **Cavagna GA, Heglund NC, and Taylor CR.** Mechanical work in terrestrial locomotion: two basic mechanisms for minimizing energy expenditure. *Am J Physiol Regulatory Integrative Comp Physiol* 233: R243–R261, 1977.
9. **Cavagna GA, Saibene FP, and Margaria R.** Mechanical work in running. *J Appl Physiol* 19: 249–256, 1964.
10. **Cavagna GA, Thys H, and Zamboni A.** The sources of external work in level walking and running. *J Physiol (Lond)* 262: 639–657, 1976.
11. **Farley CT, Blickman R, Saito J, and Taylor CR.** Hopping frequency in humans: a test of how springs set stride frequency in bouncing gaits. *J Appl Physiol* 71: 2127–2132, 1991.
12. **Farley CT, Glasheen J, and McMahon TA.** Running springs: speed and animal size. *J Exp Biol* 185: 71–86, 1993.
13. **Farley CT and Gonzalez O.** Leg stiffness and stride frequency in human running. *J Biomech* 29: 181–186, 1996.
14. **Farley CT, Houdijk HHP, Strien CV, and Louie M.** Mechanism of leg stiffness adjustment for hopping on surfaces of different stiffnesses. *J Appl Physiol* 85: 1044–1055, 1998.
15. **Farley CT and Morgenroth DC.** Leg stiffness primarily depends on ankle stiffness during human hopping on surfaces of different stiffnesses. *J Biomech* 32: 267–273, 1999.
16. **Ferris DP and Farley CT.** Interaction of leg stiffness and surface stiffness during human hopping. *J Appl Physiol* 82: 15–22, 1997.
17. **Ferris DP, Liang K, and Farley CT.** Runners adjust leg stiffness for their first step on a new running surface. *J Biomech* 32: 787–794, 1999.
18. **Ferris DP, Louie M, and Farley CT.** Running in the real world: adjusting leg stiffness for different surfaces. *Proc R Soc Lond B Biol Sci* 265: 989–994, 1998.

19. **He J, Kram R, and McMahon TA.** Mechanics of running under simulated low gravity. *J Appl Physiol* 71: 863–870, 1991.
20. **Hill AV.** The dimensions of animals and their muscular dynamics. *Sci Prog* 38: 209–230, 1950.
21. **Kram R.** Muscular force or work: what determines the metabolic energy cost of running? *Exerc Sport Sci Rev* 28: 138–143, 2000.
22. **Kram R and Powell J.** A treadmill-mounted force platform. *J Appl Physiol* 67: 1692–1698, 1989.
23. **Kram R and Taylor CR.** Energetics of running: a new perspective. *Nature* 346: 265–267, 1990.
24. **Lejeune TM, Willems PA, and Heglund NC.** Mechanics and energetics of human locomotion on sand. *J Exp Biol* 201: 2071–2080, 1998.
25. **McGeer T.** Passive bipedal running. *Proc R Soc Lond B Biol Sci* 240: 107–134, 1990.
26. **McMahon TA.** Spring-like properties of muscles and reflexes in running. In: *Multiple Muscle Systems: Biomechanics and Movement Organization*, edited by Winters JM and Woo SL-Y. New York: Springer-Verlag, 1990, p. 578–590.
27. **McMahon TA and Cheng GC.** The mechanics of running: how does stiffness couple with speed? *J Biomech* 23: 65–78, 1990.
28. **McMahon TA and Greene P.** Fast running tracks. *Sci Am* 239: 148–163, 1978.
29. **McMahon TA and Greene PR.** The influence of track compliance on running. *J Biomech* 12: 893–904, 1979.
30. **McMahon TA, Valiant G, and Frederick EC.** Groucho running. *J Appl Physiol* 62: 2326–2337, 1987.
31. **Roberts TJ, Kram R, Weyand PG, and Taylor R.** Energetics of bipedal running. I. Metabolic cost of generating force. *J Exp Biol* 201: 2745–2751, 1998.

